



 Cite this: *RSC Adv.*, 2021, 11, 22983

# Synthesis and characterization of a novel magnetic porous carbon coated with poly(*p*-phenylenediamine) and its application for furfural preconcentration and determination in baby food and dry milk powder samples

 Seyedeh Dorsa Davari,<sup>a</sup> Mohammad Rabbani,<sup>b</sup>  Afshin Akhondzadeh Basti<sup>c</sup> and Mohammad Kazem Koohi<sup>d</sup>

The aim of the current research is to develop a MSPE method for the determination of furfural in baby food and dry milk samples. In this regard, a novel magnetic porous carbon composite coated with poly(*p*-phenylenediamine) was fabricated, characterized, and then applied to the preconcentration/extraction of furfurals from baby food and dry milk powder samples. Initially, magnetic nanoparticles (Fe<sub>3</sub>O<sub>4</sub>) were synthesized, and then coated with a metal–organic framework layer named MIL-101(Fe). Afterward, the magnetic MIL-101(Fe) was subjected to calcination under a nitrogen atmosphere and magnetic porous carbon was achieved. Finally, a layer of poly(*p*-phenylenediamine) was coated on the magnetic porous carbon. The structure of the nanocomposite was investigated with various methods, including FT-IR spectroscopy, electron microcopies (SEM and TEM), VSM, and XRD. The fabricated nanocomposite was applied in magnetic solid-phase extraction of furfural and hydroxymethyl furfural and their determination with liquid chromatography. The effect of experimental variables was explored by using an experimental design approach. The LODs and linear range for the target furfurals were 1.0–2.0 μg kg<sup>-1</sup> and 3.0–500 μg kg<sup>-1</sup>, respectively. The method's repeatability was explored using RSD values and was found to be in the range of 5.2–6.4% (one-day, *n* = 5) and 9.1–10.8% (day to day, *n* = 3). Eventually, this new method was employed for the extraction/quantification of target compounds in baby food and dry milk powder samples.

Received 18th January 2021

Accepted 8th June 2021

DOI: 10.1039/d1ra00444a

[rsc.li/rsc-advances](http://rsc.li/rsc-advances)

## 1. Introduction

Furfural (F) and hydroxymethyl furfural (HMF), as cyclic aldehyde compounds, are formed during the heat treatment of foods. F and HMF are the decomposition products of pentose and hexose, respectively.<sup>1,2</sup> Sugar decomposition, caramelization, and the Maillard reaction are the three primary reactions in the formation process of furfurals. In fact, F and HMF are the intermediate products of the Maillard reaction and can undergo further decarboxylation, oxidation, dehydration, and reduction reactions to produce melanoidins as the final Maillard products.<sup>3,4</sup> Furfurals are mutagenic and exhibit a DNA strand-breaking effect.<sup>5</sup>

Although these compounds are found in untreated foods, their concentration can be increased during heat processing and they can be utilized as a valuable indicator for evaluation of heat damage in foods.<sup>6</sup> Baby formulas contain vitamin A, iron, and lactose compounds, which enhance the probability of the Maillard reaction occurring in them.<sup>7</sup>

It has been legislated by the European Union that the HMF concentration of honey after processing/blending should be less than 40 mg kg<sup>-1</sup>.<sup>8</sup> The mentioned pollutants are evaluated as nutritional deterioration and heat damage tools in honey, fruit juices, and milk-based infant formula, which are employed to prepare infant and baby food.<sup>3</sup>

Various extraction/analytical methods such as spectroscopy,<sup>9</sup> solid-phase extraction-chromatography-mass spectrometry (SPE-GC-MS),<sup>10</sup> SPE-LC-MS,<sup>11</sup> and SPE-LC-MS/MS<sup>12</sup> have been reported for the quantification of F and HMF in foods. Because of the nature of a food matrix and the low levels of F and HMF in the food samples, a sample preparation step is vital, which increases the method sensitivity. In this regard, the development of a simple, facile, precise, and accurate extraction method before furfural quantification is a very significant issue.

<sup>a</sup>Department of Food Science and Technology, Tehran North Branch, Islamic Azad University, Tehran, Iran

<sup>b</sup>Department of Marine Chemistry, Faculty of Marine Science and Technology, North Tehran Branch, Islamic Azad University, Tehran, Iran. E-mail: m.rabbani.iau@gmail.com; Tel: +98 22173060

<sup>c</sup>Department of Food Hygiene, Faculty of Veterinary Medicine, University of Tehran, Tehran, Iran

<sup>d</sup>Department of Comparative Sciences, Faculty of Veterinary Medicine, University of Tehran, Tehran, Iran


A new format of solid-phase extraction (SPE) named magnetic-SPE (MSPE), based on magnetic nanoparticles/composites, is widely employed in the sample preparation process.<sup>13–16</sup> In the MSPE method, adsorbents with superparamagnetic features are applied that can be isolated from the extraction medium *via* magnetic separation, and so there is no need for a filtration/centrifugation step.<sup>17</sup> Owing to the superparamagnetic properties, magnetic adsorbents tend to form aggregates, which decreases their performance during the extraction process. Besides, bare magnetic nanoparticles do not have suitable functional moieties. Accordingly, the modification of MNPs and the fabrication of their composites are suggested.<sup>18–20</sup> Functionalization of MNPs can be accomplished by various materials, like metal–organic framework (MOFs). These materials, a unique class of porous compounds, are constructed from metallic centers and organic bridging ligands. Magnetic porous carbons (MPCs) as a group of unprecedented materials can be derived from MOFs as precursors in a one-step carbonization process.<sup>19</sup> In the carbonization procedure of some MOFs, the metallic parts aggregate producing magnetic nanoparticles (MNPs) and the linkers convert to a porous carbon backbone that embeds the MNPs.<sup>20</sup> This approach does not need additional carbon precursors. The resultant composite benefits from the superparamagnetic features of magnetic NPs, and the excellent characteristics of MPCs (chemical stability, high surface area) and for the MSPE method. The MNPs encapsulated in the carbon (MPC) prevent the agglomeration of these particles and enhance their stability in harsh chemical conditions.<sup>21</sup> Moreover, compared to non-magnetic nanocomposites such as graphene and carbon nanotubes, MPCs can be magnetically separated from the extraction media, providing faster and simpler separation.<sup>22</sup>

The aim of the current research is to develop a MSPE method for the determination of furfural in baby food and dry milk samples. In this way, a novel magnetic porous carbon composite coated with poly(*p*-phenylenediamine) (PPDA) was synthesized and applied for preconcentration/determination of furfurals in baby food and dry milk powder samples. At first, Fe<sub>3</sub>O<sub>4</sub> nanoparticles were synthesized and then were coated with a MOF layer of the type MIL-101(Fe). After that, the magnetic MIL-101(Fe) underwent calcination under an N<sub>2</sub> atmosphere, and a magnetic porous carbon (MPC) was achieved. Finally, *p*-phenylenediamine was polymerized on the MPC surface *via* oxidative polymerization. Furfurals are polar compounds, and hence a coating layer such as PPDA is necessary to improve their extractability from the aqueous medium *via*  $\pi$ – $\pi$  stacking,  $\pi$ –cation interaction, and hydrogen bond formation. To the best of the authors' knowledge, there is no report on the synthesis and utilization of MPC@poly(*p*-phenylenediamine) (MPC@PPDA) for the magnetic solid phase extraction of furfural compounds from baby food and dry milk powder samples.

## 2. Experimental

### 2.1. Reagents and solutions

LC-grade acetonitrile and methanol, 2-propanol, ethyl acetate, ethanol, acetone, FeCl<sub>3</sub>·6H<sub>2</sub>O, 1,4-benzene dicarboxylic acid

(H<sub>2</sub>BDC), FeCl<sub>3</sub>, potassium hexacyanoferrate, *p*-phenylenediamine (PDA), ammonium persulfate (APS), ammonium hydroxide (28% w/v), sodium hydroxide, NaCl, zinc acetate dihydrate (Zn(OAc)<sub>2</sub>·2H<sub>2</sub>O), acetic acid (HOAc), and *N,N*-dimethylformamide (DMF) were obtained from Merck (Darmstadt, Germany). Deionized water (DI) was prepared by utilizing a Milli-Q system from Millipore (MA, USA). Baby food and dry milk powder samples were purchased from Tehran supermarkets/drug stores (Tehran, Iran) and refrigerated at 4 °C before analysis.

F and HMF (analytical-grade) were obtained from Sigma-Aldrich (Germany). Stock solutions of F and HMF (1000 µg mL<sup>-1</sup>) were prepared in methanol. Working mixed solutions of furfurals were prepared daily by diluting appropriate volumes of the stock solutions in DI water. Carrez solutions I and II were used for sample preparation. Carrez solution I was fabricated by dissolving 10.6 g K<sub>3</sub>[Fe(CN)<sub>6</sub>] in 100 mL DI water. To prepare Carrez solution II, in brief, 21.9 g Zn(OAc)<sub>2</sub> along with 3 mL HOAc were mixed in a 100 mL volumetric flask, and then its volume was adjusted with DI water.

### 2.2. Instruments

Chromatographic separation/quantification was accomplished on a Knauer HPLC (Wellchrom model) system (Berlin, Germany) consisting of the following: a smart-line pump 1000, a multiple solvent delivery unit, a 6-port/3-channel injection valve (Knauer, Germany), a K-5020 vacuum degasser, and a smart-line 2500UV-Vis detector. Separation of F and HMF were performed on an ODS-H C18 capital HPLC column (Scotland, UK, 250 × 4.6 mm I.D., 5 µm). A mixture of DI water and acetonitrile (95 : 5 v/v) with a flow rate of 1.0 mL min<sup>-1</sup> was employed as the mobile phase. The mobile phase was filtered *via* a Millipore 0.22 µm membrane filter before use. The injection volume and detection wavelength were 100 µL and 285 nm, respectively. The retention time for HMF and F was 10.2 and 15 min, respectively.

FT-IR spectra were obtained by employing a Bomem MB-Series spectrophotometer (USA). Magnetic features of the fabricated adsorbents were recorded on a vibrating sample magnetometer (VSM) system (Kashan Kavir; Iran) at room temperature by applying a 1 T magnetic field. X-ray diffraction (XRD) patterns were recorded on a Philips-PW 12C diffractometer system (Amsterdam, The Netherlands) consisting of a copper K $\alpha$  radiation source. The morphology study was conducted on a scanning electron microscope (SEM) of the type KYKY-3200 (Beijing, China, Zhongguancun Beijing, China). The transmission electron microscopy (TEM) assay was accomplished on Zeiss-EM10C-100 kV apparatus (Carl Zeiss, Germany).

### 2.3. Fabrication of the nanoadsorbent

MNPs were fabricated *via* a chemical coprecipitation process according to a previous work.<sup>23</sup> To synthesize magnetic MIL-101(Fe), 0.5 g MNPs and 3.4 g FeCl<sub>3</sub>·6H<sub>2</sub>O were added to 50 mL DMF and stirred for 45 min (mixture 1). Afterward, 1.0 g H<sub>2</sub>BDC was added to 50 mL DMF (mixture 2). After that,



mixtures 1 and 2 were mixed in a Teflon autoclave, and the reaction was accomplished at 110 °C for 24 h.<sup>24</sup> Finally, the MIL-101(Fe)/MNP composite was isolated from the extraction medium magnetically and it was washed with DI water and ethanol to discard the unreacted reagents and then dried at ambient temperature. MIL-101(Fe) was prepared with the same procedure in the absence of magnetite.

In the next step, the MIL-101(Fe)/MNPs were carbonized under a nitrogen atmosphere (600 °C, 2 h), and a MPC composite was achieved. Finally, a polymer layer of the type poly(*p*-phenylenediamine) (PPDA) was coated on the MPC *via* oxidative polymerization. In this regard, 0.5 g MPC and 2.16 PDA were suspended in 150 mL 0.2 mol L<sup>-1</sup> HCl solution in an ice bath (4 °C). Afterwards, 5.4 g APS was dissolved in 20 mL DI water and was added to the reaction mixture drop by drop in the ice bath for 30 min. The reaction was conducted for 24 h at 4 °C.<sup>25</sup> Finally, to stop the reaction, acetone was added to the mixture, and the MPC@PPDA precipitate was gathered and

washed with water and methanol seven times to discard the unreacted reagents and finally dried at 50 °C for 12 h.

#### 2.4. Sample pretreatment

In brief, 10 mL DI water was mixed with 10 g of each sample in a conical tube and then spiked with F and HMF. After that, the mixture was stirred thoroughly for 5 min to achieve a homogeneous sample. In the next step, 4 g of the homogeneous sample was transferred to another conical tube, and 9 mL 0.02 mol L<sup>-1</sup> sodium hydroxide solution was added to hydrolyze the sample. Afterward, the pH of the solution was adjusted to 3 and the mixture of Carrez solution I (2 mL) and Carrez solution II (2 mL) was added to the sample to separate the protein content as a precipitate,<sup>26</sup> and it was shaken for 2 min. Next, the mixture was centrifuged at 4000 rpm (5 min), and the supernatant was gathered, and then filtered by a Millipore 0.45 μm cellulose acetate membrane filter.

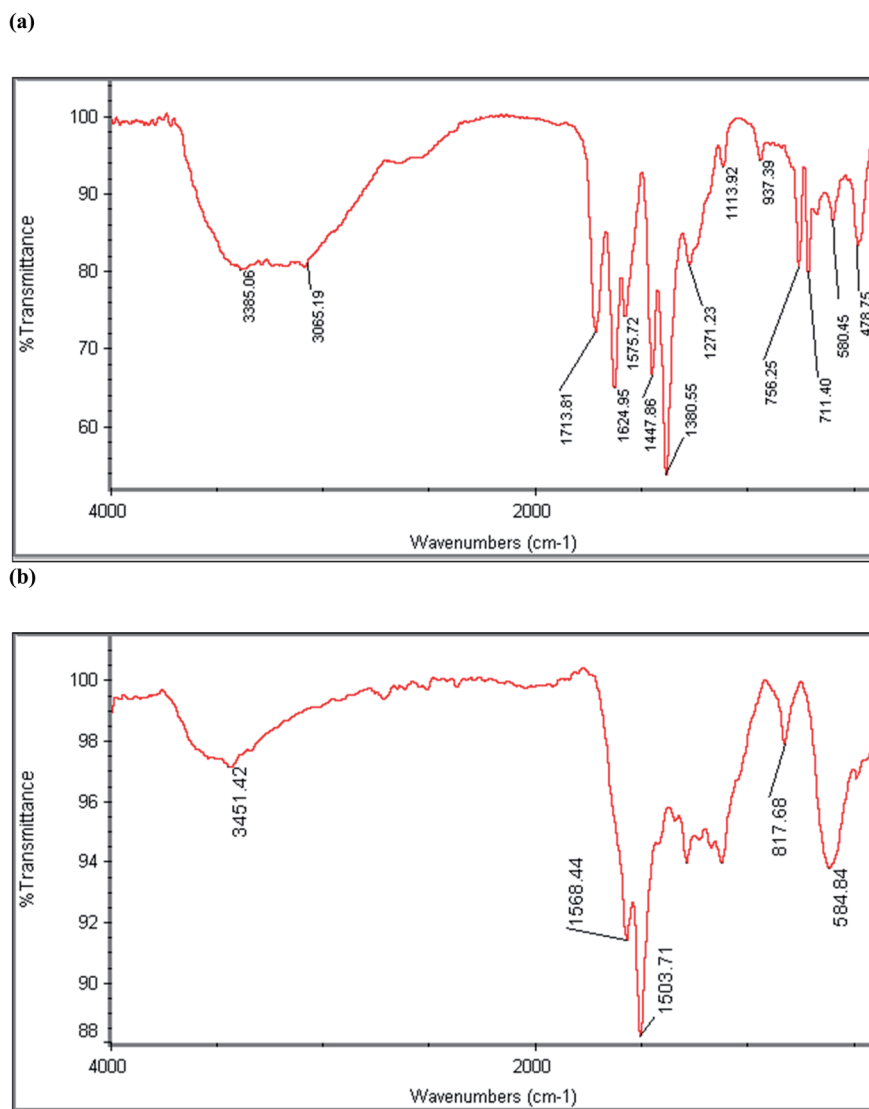


Fig. 1 FT-IR spectra of (a) MIL-101(Fe)/MNPs and (b) the MPC@PPDA nanocomposite.



## 2.5. Extraction/separation process

At first, 40 mg MPC@PPDA was dispersed into 25 mL 0.1 mg L<sup>-1</sup> furfural solution/real samples containing 15% w/v NaCl. After adjusting the pH of the solution to 5.6, it was shaken for 16.0 min to extract the analytes. After that, the MPC@PPDA was isolated from the extraction medium magnetically. 20 mL of the upper solution was discarded, and then the remaining solution (5 mL) was transferred into a conical vial. The nanoadsorbent was separated again, and finally, the remaining solution was decanted, and 140 μL methanol was added to desorb the furfurals under fierce vortexing (3.0 min at 3000 rpm). Finally, the MPC was isolated magnetically from the eluent and injected into the HPLC instrument for quantification.

## 3. Results

### 3.1. Characterization assays

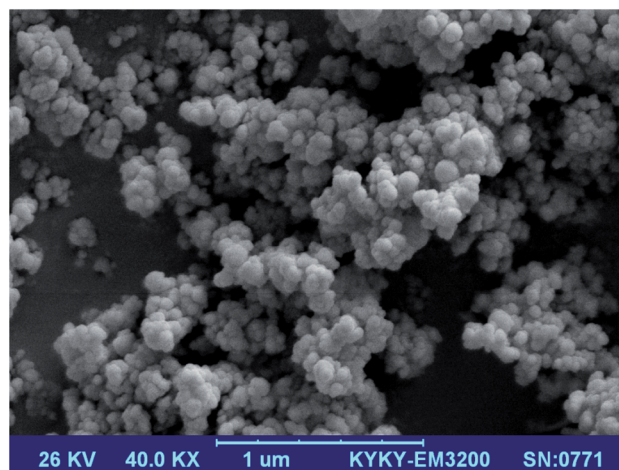
To study the functional groups of the MIL-101(Fe)/MNPs and MPC@PPDA nanocomposites, FT-IR spectroscopy was applied (Fig. 1). In the spectrum of MIL-101(Fe)/MNPs (Fig. 1a), the characteristic absorption bands of Fe–O (580 cm<sup>-1</sup>), C–O–C (1380 and 1624 cm<sup>-1</sup>), C=O (1713 cm<sup>-1</sup>), and O–H (3385 cm<sup>-1</sup>) were observed, which confirms the synthesis of MIL-101(Fe) and magnetite. In the spectrum of MPC@PPDA (Fig. 1b), the presence of the absorption bands at 584 cm<sup>-1</sup> (Fe–O), 1301 cm<sup>-1</sup> (C–N), 1500–1600 cm<sup>-1</sup> (C=N, C=C), and 3451 cm<sup>-1</sup> (N–H) confirms the presence of MNPs and PPDA polymer in the fabricated material.

The morphology of the MPC@PPDA nanocomposite was characterized by TEM and SEM methods. As represented in the SEM image in Fig. 2a, MPC@PPDA shows a three-dimensional porous structure, with spherical particles (diameter, *ca.* 50 nm). As depicted in the TEM micrograph (Fig. 2b), the MPC@PPDA nanocomposite has a highly porous structure and shows no noticeable aggregation. The average particle size according to the TEM method was 25 nm. This difference in the particle sizes between SEM and TEM can be related to the lower resolution of the SEM technique compared to TEM.<sup>27</sup>

To study the crystalline structure of the MIL-101(Fe)/MNPs and MPC@PPDA nanocomposites, their XRD patterns were recorded in the 2θ region of 1–80° (Fig. 3a and b). In the XRD pattern of the MIL-101(Fe)/MNPs, the diffraction peaks at 2θ = 9, 16.5, and 18.6 correspond to MIL-101(Fe). Besides, the characteristic peaks of magnetite (2θ = 30.2, 35.6, 43.4, 57.2, 63.0, and 74.5) are observable in the MIL-101(Fe)/MNPs pattern. The diffraction peaks at 2θ = 30.5, 35.8, 43.3, 57.3, 62.9, and 74.1 in the pattern of MPC@PPDA correspond to Fe<sub>3</sub>O<sub>4</sub> crystals and confirm the presence of MNPs in this material.

In the next step, the magnetic characteristics of the MNPs and MPC@PPDA were studied and compared using the VSM method. As depicted in Fig. 3c, the VSM curves showed no magnetic hysteresis loops, which can be attributed to their superparamagnetic properties. The saturation magnetization of the MNPs and MPC@PPDA are 58 and 38 emu g<sup>-1</sup>, respectively, which is sufficient for magnetic isolation. The decrease in the magnetization of MPC@PPDA compared to the MNPs is owing

(a)



(b)

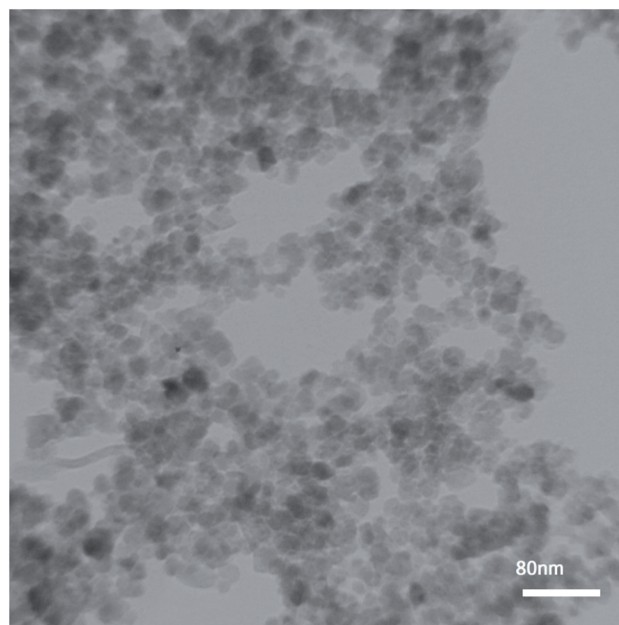


Fig. 2 (a) SEM image of the MPC@PPDA nanocomposite, and (b) TEM micrograph of the MPC@PPDA nanocomposite.

to the formation of the carbon skeleton and PPDA polymer layer in the final composite, which act as a shield.

### 3.2. Optimization

**3.2.1. Selection of the nanoadsorbent.** To select the best nanoadsorbent, various fabricated materials such as MNPs, MIL-101(Fe), MIL-101(Fe)/MNPs, MPC, and MPC@PPDA were evaluated in the extraction of F and HMF. As illustrated in Fig. 4a, MPC@PPDA exhibited the best extraction performance towards furfural compounds among the tested materials. The improved performance of MPC@PPDA can be attributed to the



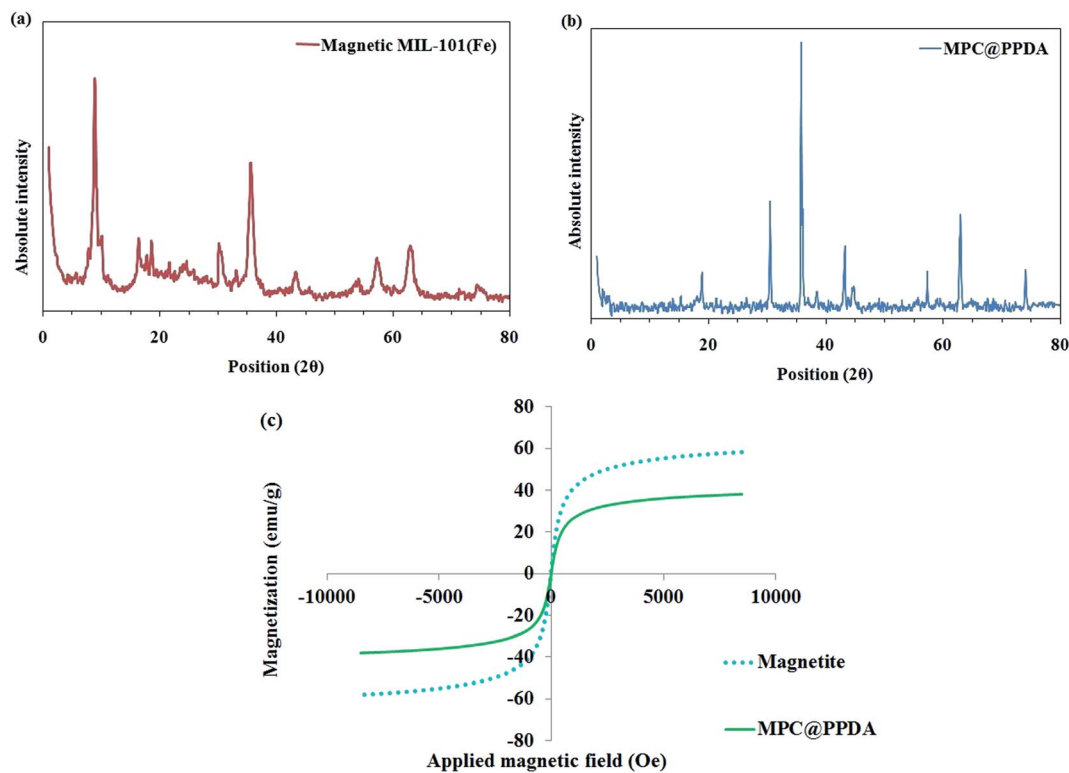


Fig. 3 XRD patterns of (a) MIL-101(Fe)/MNPs and (b) the MPC@PPDA nanocomposite; (c) VSM curves of the MNPs and MPC@PPDA.

presence of PPDA and the carbon skeleton. F ( $\log K_{OW} = 0.41$ ) and HMF ( $\log K_{OW} = -0.39$ ) are polar compounds, and a coating layer such as PPDA can improve their extractability from the aqueous medium *via*  $\pi$ - $\pi$  stacking,  $\pi$ -cation

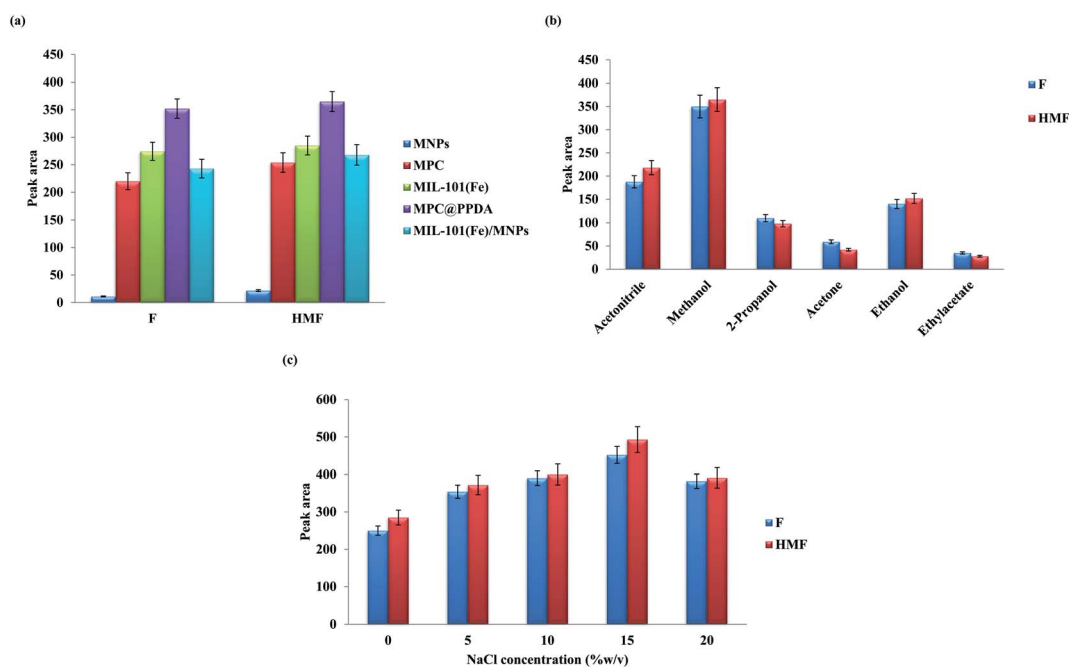


Fig. 4 (a) Effect of adsorbent type. Extraction conditions: solution pH, 5.0; sorption time, 20 min; adsorbent dose, 50 mg; eluent type, methanol; eluent volume, 150  $\mu$ L; desorption time, 2 min; NaCl concentration, 10% w/v. (b) Effect of eluent type. All conditions are similar to (a), except for adsorbent type. (c) Effect of salt concentration on the extraction performance. All conditions are similar to (b) except for the eluent type, which is methanol.

Table 1 Experimental variables and their studied ranges

	Level			Star points ( $\alpha = 2$ )	
	Lower	Central	Upper	$-\alpha$	$+\alpha$
A: pH	3.0	4.5	6.0	1.5	7.5
B: Sorption time (min)	10.0	15.0	20.0	5.0	25.0
C: Eluent volume ( $\mu\text{L}$ )	100	150	200	50	250
D: MPC@PPDA dose (mg)	20.0	30.0	40.0	10.0	50.0

interaction, and hydrogen bond formation. Besides, the carbon skeleton of MPC@PPDA can interact with the aromatic ring of furfurals *via*  $\pi$ - $\pi$  stacking. Moreover, the magnetic feature of MPC@PPDA facilitates the separation/extraction process. Accordingly, MPC@PPDA was selected as the best adsorbent.

**3.3.2. Effect of eluent type and salt addition.** The selection of a suitable elution solvent in the MSPE process is very significant due to its effect on the extraction efficiency. The eluent should have a high tendency towards the target analytes and also should be compatible with the analytical system. Accordingly, various extraction solvents, including methanol, ethanol, acetonitrile, acetone, 2-propanol and ethyl acetate, were tested to select the best eluent (Fig. 4b). The results

revealed that methanol has the best performance for eluting the target analytes and hence it was used in the remaining assays.

The effect of salt concentration on the extractability of F and HMF was studied by addition of various amounts of NaCl (0–20% w/v) to the sample solution (Fig. 4c). Salt addition can alter the solubility and diffusion rate of the analytes in the solution. The results exhibited that the extraction performance of furfural compounds increases with the addition of salt up to 15% w/v, and then a decrease in the efficiency was observed. The increase in extraction efficiency can be associated with the salting-out effect. The reduction of the extraction performance beyond 15% w/v can be related to the increase of the solution viscosity.<sup>28</sup> Besides, at a higher NaCl value, the active sites of MPC@PPDA will be saturated by the coexisting ions.<sup>28</sup>

**3.2.3. Central composite design.** The effect of four parameters, namely pH of the solution, adsorption time, eluent volume, and MPC@PPDA amount, on the extraction performance of furfurals was explored and optimized *via* the central composite design (CCD) method. In this regard, Design-Expert 7.0.0 software was utilized. Accordingly, 30 experiments were designed by choosing six replicates as the center points and according to the  $N = 2^f + 2f + C_0$  equation ( $N$ , number of experiments;  $f$ , variables number;  $C_0$ , center points number).<sup>29–31</sup> The range of studied variables is tabulated in Table 1. The geometric mean of response was applied as

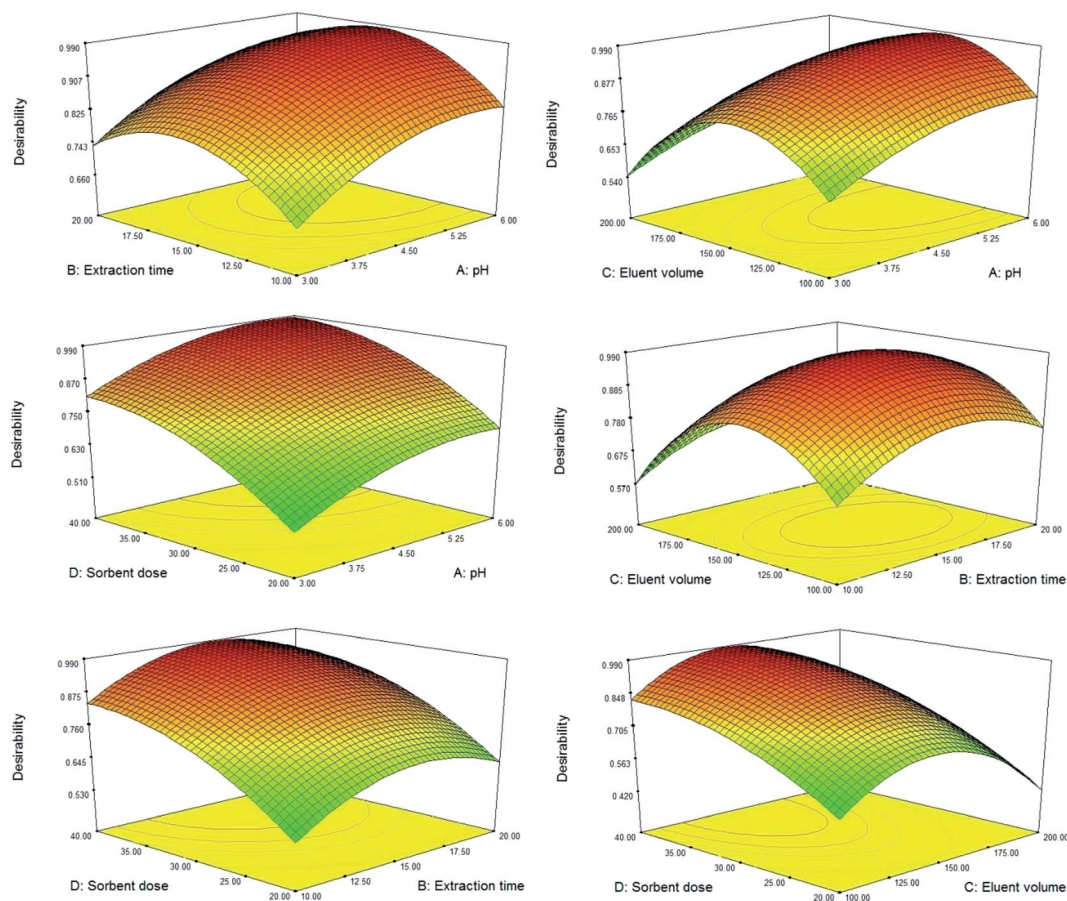


Fig. 5 3D response surface plots of the CCD study.



Table 2 Analytical features of the MSPE-HPLC-UV method<sup>a</sup>

Analyte	LOD	LOQ	Linear range	$R^2$	EF <sup>b</sup>	RSD (%) (within day) <sup>c</sup>	RSD (%) (between day) <sup>c</sup>
F	1.0	3.0	3.0–400	0.9971	125	5.2	10.8
HMF	2.0	7.0	7.0–500	0.9945	113	6.4	9.1

<sup>a</sup> All concentrations are based on  $\mu\text{g kg}^{-1}$ . <sup>b</sup> Enhancement factor. <sup>c</sup> Relative standard deviations ( $n = 5$  samples for within day and  $n = 3$  days for between day) were obtained at a  $20 \mu\text{g kg}^{-1}$  level of the furfurals.

a proper response to explore each factor effect and the possible interactions.

The results of the CCD study exhibited good accordance with the quadratic polynomial model. ANOVA was applied to determine the significant parameters and their possible interactions, and to construct the model. The results of ANOVA exhibited that MPC@PPDA has the highest significant effect on the extraction performance. The pH of the sample and the eluent volume were the second and third most significant variables and extraction time showed a non-significant effect on the extraction performance. A model  $p$ -value lower than 0.0001 was observed, which proves that the suggested model is significant and implies that there is only a 0.01% chance that a “Model  $F$ -value” this large could occur due to noise. Moreover, the  $p$ -value of the lack of fit is 0.0674 ( $0.05 <$ ), which confirms that this value is non-significant relative to the pure error.<sup>29–31</sup>

The best extraction efficiency was obtained under the following experimental condition: a pH value of 5.6, an MPC@PPDA amount of 40 mg, an extraction time of 16.0 min, and an eluent volume of 140  $\mu\text{L}$  (Fig. 5). As illustrated in Fig. 5, all the parameters were optimized properly in the studied domain and exhibit a curvature. Under these conditions, the desirability value is equal to 0.987. Nanostructured adsorbents such as MPC@PPDA benefit from a high surface area and short analyte diffusion route that leads to higher extraction performance and faster extraction kinetics compared with conventional adsorbents. The extraction efficiency of F and HMF was improved by enhancing the eluent volume up to 140  $\mu\text{L}$ , and then a decrease was observed in the enhancement factors owing to the dilution effect.

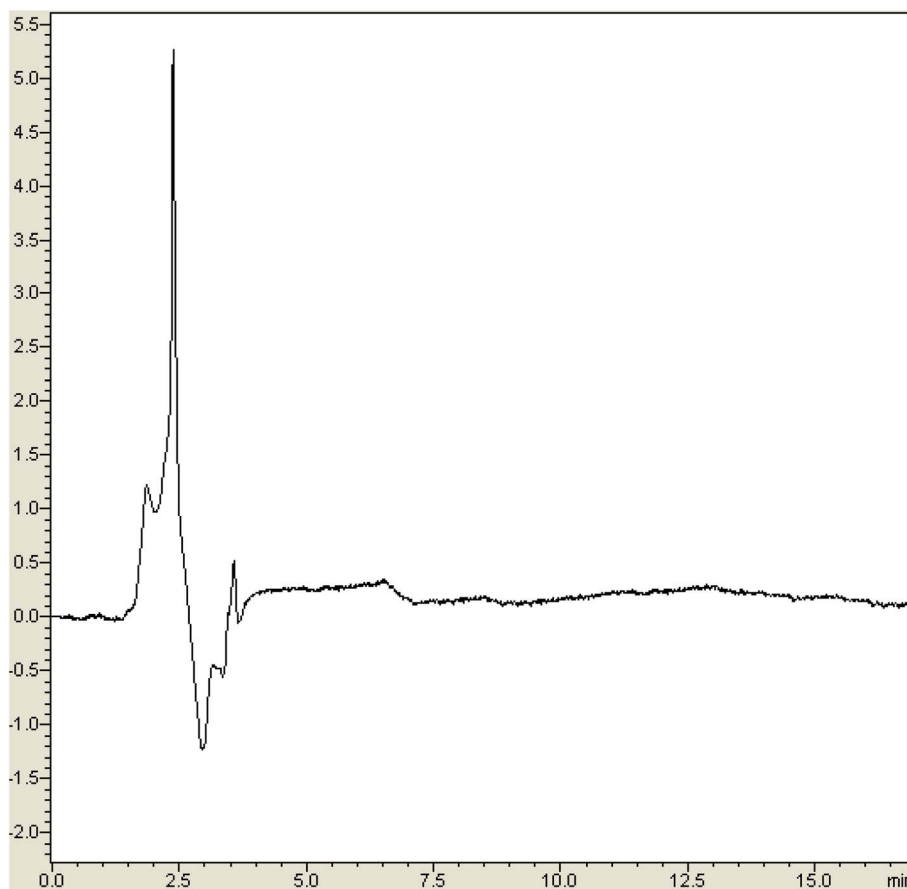


Fig. 6 The chromatogram of a non-spiked sample solution, after performing the MSPE process.



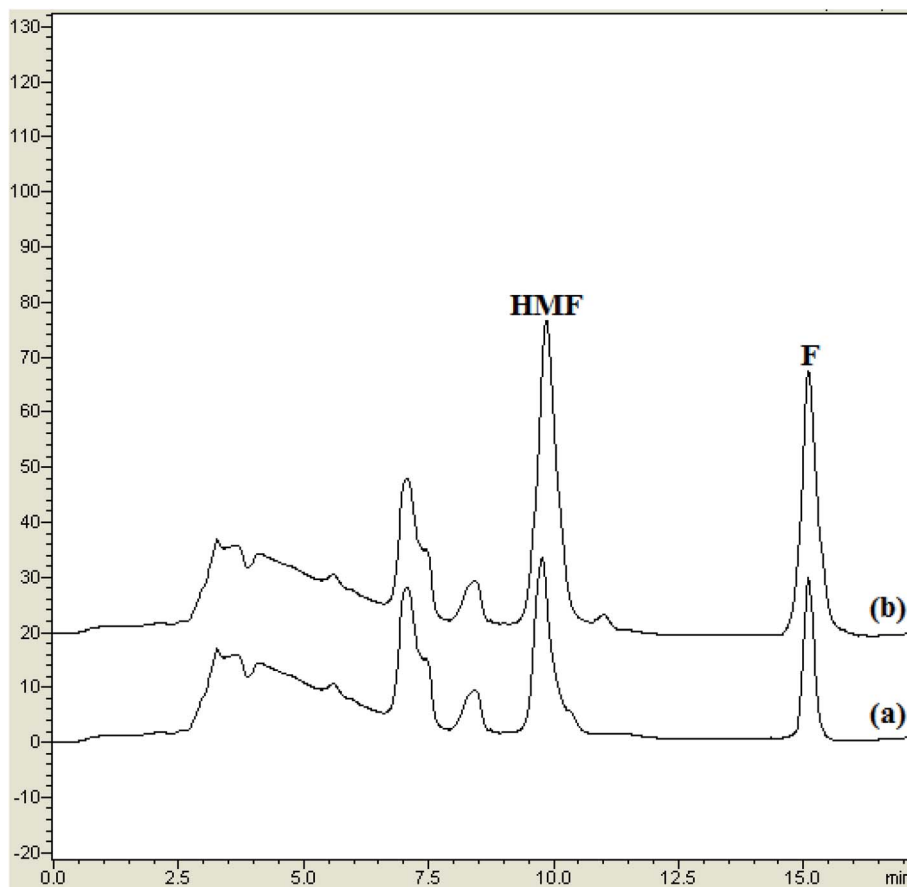


Fig. 7 The chromatograms of: (a) non-spiked dry milk 3, and (b) spiked dry milk 3 at  $25.0 \mu\text{g kg}^{-1}$  of HMF and  $10.0 \mu\text{g kg}^{-1}$  of F, after performing the MSPE process.

### 3.3. Analytical features and application

Analytical features of the new method, including the limit of detection (LOD,  $S/N = 3$ ), the limit of quantification (LOQ,  $S/N = 10$ ), enhancement factor (EF), linear range, and precision, were explored (Table 2). Fig. 6 represents the chromatogram of a non-spiked (blank) sample solution, after performing the MSPE process for calculating the LODs based on the  $S/N$  ratio of 3. The LOD and linear range for the target furfurals were  $1.0\text{--}2.0 \mu\text{g kg}^{-1}$  and  $3.0\text{--}500 \mu\text{g kg}^{-1}$ , respectively. The precision of the method was explored as RSD values.

RSD was calculated using eqn (1):

$$\text{RSD (\%)} = \frac{\text{SD}}{\bar{X}} \times 100 \quad (1)$$

where SD represents the standard deviation and  $\bar{X}$  is the average of measurement.

Based on the above equation, the RSDs were obtained in the range of 5.2–6.4% (one-day,  $n = 5$ ) and 9.1–10.8% (day to day,  $n = 3$ ). EF was determined by dividing the slope of the calibration plot after preconcentration by the slope of the calibration plot before performing the extraction process.<sup>28</sup>

Baby food and dry milk samples were analyzed to reveal the applicability of the method. The concentration of F and HMF was computed using the calibration equation of each of them

and using the spiking method. The relative recovery was calculated using eqn (2):

$$\text{RR\%} = \frac{C_{\text{found}} - C_{\text{real}}}{C_{\text{added}}} \times 100 \quad (2)$$

Table 3 The results of dry milk and baby food sample analysis

Sample	Analyte	Real value	Added	Found $\pm$ SD <sup>b</sup>	Recovery (%)
Dry milk 1	F	10.5	10.0	$19 \pm 1.7$	85
	HMF	251	250	$453 \pm 47$	81
Dry milk 2	F	ND <sup>a</sup>	10.0	$9.1 \pm 0.8$	91
	HMF	25.8	25.0	$52.1 \pm 4.4$	105
Dry milk 3	F	7.5	10.0	$17.2 \pm 1.2$	97
	HMF	25.3	25.0	$51.3 \pm 3.8$	104
Dry milk 4	F	ND	10.0	$9.5 \pm 1.0$	95
	HMF	16.3	15.0	$32.1 \pm 2.8$	105
Baby food 1	F	210	200	$401 \pm 28$	96
	HMF	1503	1000	$2402 \pm 100$	90
Baby food 2	F	195	200	$380 \pm 31$	93
	HMF	1204	1000	$2109 \pm 125$	91
Baby food 3	F	440	400	$790 \pm 51$	88
	HMF	1095	1000	$2120 \pm 140$	102
Baby food 4	F	590	500	$1028 \pm 70$	88
	HMF	7810	1000	$8925 \pm 405$	111

<sup>a</sup> All concentrations are based on  $\mu\text{g kg}^{-1}$ . <sup>b</sup> Relative recovery.





Table 4 Analytical features of the MSPE-HPLC-UV method on comparison with the former works

Analyte	Method	Linear range <sup>a</sup>	R <sup>2</sup>	LOD <sup>a</sup>	LOQ <sup>a</sup>	RSD (%)	Ref.
F	DLLME <sup>b</sup> -HPLC-UV	1.0–200	0.99<	0.7	2.4	3.9	1
HMF				1.8	5.9	4.9	
F	LLE-HPLC-UV	110–22 220	—	133	—	12.7	2
HMF				67		4.4	
F	DLLME-HPLC-UV	0.2–200	0.9902	1.3	4.4	4.7	3
HMF			0.9915	2.1	6.7	5.1	
HMF	SPE-LC-MS <sup>c</sup>	50–2000	0.99<	5.0	—	≤5.1	11
HMF	HPLC-UV	10–200 000	—	30.0	—	<2.7	32
F	HPLC-UV	140–3000	0.9999	3.5	11.6	—	33
HMF		80–10 000		8.0	27.0		
F	LLE-HPLC-DAD <sup>d</sup>		0.9991	1.1 <sup>e</sup>	3.7 <sup>e</sup>	1.52	34
HMF			0.9998	4.8 <sup>e</sup>	15.9 <sup>e</sup>	1.08	
F	MSPE-HPLC-UV	3.0–400	0.9971	1.0	3.0	5.2	This study
HMF		7.0–500	0.9945	3.0	7.0	6.4	

<sup>a</sup> All concentrations are based on  $\mu\text{g kg}^{-1}$ . <sup>b</sup> Dispersive liquid-liquid microextraction. <sup>c</sup> Mass spectrometry. <sup>d</sup> Diode array detection  $\mu\text{g L}^{-1}$ . <sup>e</sup>  $\mu\text{g L}^{-1}$ .

In this equation  $C_{\text{found}}$ ,  $C_{\text{real}}$ , and  $C_{\text{added}}$  represent the concentration of furfurals in the spiked samples, the concentration of furfurals in the non-spiked sample, and the spiked level for the real sample, respectively.<sup>28</sup> Fig. 7 depicts the chromatograms of non-spiked dry milk 3, and spiked dry milk 3 at  $25.0 \mu\text{g kg}^{-1}$  of HMF and  $10.0 \mu\text{g kg}^{-1}$  of F, after performing the MSPE process. As exhibited in Table 3, the relative recovery and precision were obtained in the ranges of 81–111% and 4.2–10.5%, which are desirable. These results suggest that the MSPE method is reliable and precise and provides a matrix-free analysis.

### 3.4. Comparison study

The analytical properties of the current method were compared with some former methods for furfural separation/determination (Table 4). As summarized in this table, the new method provides a wide linear range, low LODs and LOQs, acceptable precision, and high EFs compared to the other methods. The obtained LOD values are lower than or comparable to the reported values. Besides, the LOD values are low enough to satisfy the permissible thresholds established by the European Union for furfurals in food samples. Moreover, this method is simple and requires low levels of organic solvent.

## 4. Conclusion

Herein, a novel MPC composite coated with poly(*p*-phenylenediamine) was synthesized and applied for preconcentration/determination of furfurals in baby food and dry milk powder samples. At first,  $\text{Fe}_3\text{O}_4$  nanoparticles were synthesized and then were coated with a MOF layer named MIL-101(Fe). After that, the magnetic MIL-101(Fe) was subjected to calcination under an  $\text{N}_2$  atmosphere and the MPC was achieved. Finally, *p*-phenylenediamine was coated on the MPC *via* oxidative polymerization. To the best of the authors' knowledge, there is no report on the synthesis and utilization of MPC@PPDA for the magnetic solid-phase extraction of furfural compounds from

baby food and dry milk powder samples. Due to the presence of the PPDA polymer and the carbon skeleton, polar furfural compounds can be extracted from the aqueous medium *via*  $\pi$ - $\pi$  stacking,  $\pi$ -cation interaction, and hydrogen bond formation. Moreover, the magnetic features of MPC@PPDA facilitate the separation/extraction (less than 18 min) process. Finally, the outlined method was applied to the fast separation and quantification of polar furfural compounds in baby food and dry milk samples, satisfactorily.

## Conflicts of interest

The authors declare that they have no conflict of interest.

## References

- 1 M. Madani-Tonekaboni, M. Kamankesh and A. Mohammadi, *J. Food Compos. Anal.*, 2015, **40**, 1–7.
- 2 E. Ferrer, A. Alegria, R. Farré, P. Abellán and F. Romero, *Food Chem.*, 2005, **89**, 639–645.
- 3 H. Habibi, A. Mohammadi and M. Kamankesh, *Nutr. Food Sci. Res.*, 2017, **4**, 25–32.
- 4 M. J. Antal Jr, W. S. Mok and G. N. Richards, *Carbohydr. Res.*, 1990, **199**, 91–109.
- 5 *ACS Symp. Ser.*, ed., H. Omura, N. Jahan, K. Shinohara, H. Murakami, G. R. Waller and M. S. Feather, Am. Chem. Soc., Washington, DC, 1983, vol. 215, p. 537.
- 6 B. Fallico, E. Arena and M. Zappala, *Food Chem.*, 2003, **81**, 569–573.
- 7 E. Ferrer, A. Alegria, R. Farre, P. Abellan and F. Romero, *J. Chromatogr. A*, 2002, **947**, 85–95.
- 8 *Directive 2001/110/EC of 20 December 2001*, 2001, Official Journal of the European Communities, pp. 47–52.
- 9 R. A. Motiyenko, E. A. Alekseev and S. F. Dyubko, *J. Mol. Spectrosc.*, 2007, **244**, 9–12.
- 10 E. Teixidó, F. Santos, L. Puignou and M. T. Galceran, *J. Chromatogr. A*, 2006, **1135**, 85–90.



- 11 V. Gökmen and H. Z. Şenyuva, *J. Agric. Food Chem.*, 2006, **54**, 2845–2849.
- 12 E. Teixido, E. Moyano, F. J. Santos and M. T. Galceran, *J. Chromatogr. A*, 2008, **1185**, 102–108.
- 13 S. Rezabeyk and M. Manoochchri, *RSC Adv.*, 2020, **10**, 36897–36905.
- 14 A. A. Asgharinezhad, N. Jalilian, H. Ebrahimzadeh and Z. Panjali, *RSC Adv.*, 2015, **5**, 45510–45519.
- 15 F. Abujaber, L. Avendaño, S. Jodeh, Á. Ríos, F. J. Guzmán Bernardo and R. C. Rodríguez Martín-Doimeadios, *Sep. Sci. plus*, 2018, **1**, 549–555.
- 16 J. Y. Wu, H. X. Zhang and X. T. Peng, *Sep. Sci. plus*, 2020, **3**(5), 158–166.
- 17 A. Afkhami, S. Aghajani, T. Madrakian and H. Bagheri, *Chem. Pap.*, 2020, **17**, 1–7.
- 18 M. Zeeb and H. Farahani, *Chem. Pap.*, 2018, **72**, 15–27.
- 19 W. Xia, J. Zhu, W. Guo, L. An, D. Xia and R. Zou, *J. Mater. Chem. A*, 2014, **2**, 11606–11613.
- 20 F. Maya, C. P. Cabello, R. M. Frizzarin, J. M. Estela, G. T. Palomino and V. Cerdà, *TrAC, Trends Anal. Chem.*, 2017, **90**, 142–152.
- 21 C. Yu, Y. F. Sun, X. M. Fan, Z. B. Zhao and J. S. Qiu, *Part. Part. Syst. Charact.*, 2013, **30**, 637–644.
- 22 L. Hao, C. Wang, Q. Wu, Z. Li, Z. Zang and Z. Wang, *Anal. Chem.*, 2014, **86**, 12199–12205.
- 23 A. A. Asgharinezhad, H. Ebrahimzadeh, M. Rezvani, N. Shekari and M. Loni, *Food Addit. Contam., Part A*, 2014, **31**, 1196–1204.
- 24 M. Babazadeh, R. Hosseinzadeh-Khanmiri, J. Abolhasani, E. Ghorbani-Kalhor and A. Hassanpour, *RSC Adv.*, 2015, **5**, 19884–19892.
- 25 S. Yang, D. Liu, F. Liao, T. Guo, Z. Wu and T. Zhang, *Synth. Met.*, 2012, **162**, 2329–2336.
- 26 V. Ghasemzadeh-Mohammadi, A. Mohammadi, M. Hashemi, R. Khaksar and P. Haratian, *J. Chromatogr. A*, 2012, **1237**, 30–36.
- 27 A. A. Asgharinezhad, N. Mollazadeh, H. Ebrahimzadeh, F. Mirbabaei and N. Shekari, *J. Chromatogr. A*, 2014, **1338**, 1–8.
- 28 N. Jalilian, H. Ebrahimzadeh and A. A. Asgharinezhad, *J. Chromatogr. A*, 2017, **1499**, 38–47.
- 29 H. Ebrahimzadeh, A. A. Asgharinezhad, L. Adlnasab and N. Shekari, *J. Sep. Sci.*, 2012, **35**, 2040–2047.
- 30 A. Ostovan, M. Ghaedi, M. Arabi, Q. Yang, J. Li and L. Chen, *ACS Appl. Mater. Interfaces*, 2018, **10**, 4140–4150.
- 31 A. R. Bagheri, M. Arabi, M. Ghaedi, A. Ostovan, X. Wang, J. Li and L. Chen, *Talanta*, 2019, **195**, 390–400.
- 32 L. V. I. B. K. Kalábová and V. Večerek, *J. Food Nutr. Res.*, 2006, **45**, 34–38.
- 33 M. Mesias-Garcia, E. Guerra-Hernandez and B. Garcia-Villanova, *J. Agric. Food Chem.*, 2010, **58**, 6027–6032.
- 34 B. E. Demirhan, B. Demirhan, C. Sönmez, H. Torul, U. Tamer and G. Yentür, *J. Dairy Sci.*, 2015, **98**, 818–822.

